



# Network Polymer Properties Engineered Through Polymer Backbone Dispersity and Structure

## Journal Article

### Author(s):

Raji, Ibrahim O.; Dodo, Obed J.; Saha, Nirob K.; Eisenhart, Mary; Miller, Kevin M.; [Whitfield, Richard](#) ; [Whitfield, Richard](#) ; Anastasaki, Athina; Konkolewicz, Dominik

### Publication date:

2024

### Permanent link:

<https://doi.org/10.3929/ethz-b-000670464>

### Rights / license:

[Creative Commons Attribution-NonCommercial 4.0 International](#)

### Originally published in:

Angewandte Chemie. International Edition, <https://doi.org/10.1002/anie.202315200>



# Network Polymer Properties Engineered Through Polymer Backbone Dispersity and Structure

Ibrahim O. Raji, Obed J. Dodo, Nirob K. Saha, Mary Eisenhart, Kevin M. Miller, Richard Whitfield, Athina Anastasaki, and Dominik Konkolewicz\*

**Abstract:** Dispersity ( $\mathcal{D}$  or  $M_w/M_n$ ) is an important parameter in material design and as such can significantly impact the properties of polymers. Here, polymer networks with independent control over the molecular weight and dispersity of the linear chains that form the material are developed. Using a RAFT polymerization approach, a library of polymers with dispersity ranging from 1.2–1.9 for backbone chain-length (DP) 100, and 1.4–3.1 for backbone chain-length 200 were developed and transformed to networks through post-polymerization crosslinking to form disulfide linkers. The tensile, swelling, and adhesive properties were explored, finding that both at DP 100 and DP 200 the swelling ratio, tensile strength, and extensibility were superior at intermediate dispersity (1.3–1.5 for DP 100 and 1.6–2.1 for DP 200) compared to materials with either substantially higher or lower dispersity. Furthermore, adhesive properties for materials with chains of intermediate dispersity at DP 200 revealed enhanced performance compared to the very low or high dispersity chains.

instance, the properties of polyethylene change substantially with polymer structure. Higher branching leads to low-density polyethylene with low crystallinity which is suitable for applications that require more stretchability and flexibility, while low branching and high crystallinity lead to high-density polyethylene, which makes it a better option for more rigorous heavy-duty applications where higher chemical resistance and stiffness are required. Thus, high-density polyethylene utilizes the higher rigidity imparted by crystallinity.<sup>[4–9]</sup> Recent advances in controlled and reversible deactivation polymerization methods have allowed unprecedented control over primary polymer structure.<sup>[10–15]</sup> In particular, reversible deactivation radical polymerization (RDRP) methods are among the most effective polymerization techniques for controlling the primary polymer structure. The desirability of RDRP methods arises from their ability to control the molecular weight of polymers with various functional groups, and to form complex polymers such as stars, block copolymers, and branched materials.<sup>[10,16–19]</sup> Recently, the ability to control primary chain dispersity has emerged as an active area of research focus, with techniques that control the polymer's uniformity through catalyst control, reagent design, reaction engineering, or blending of polymers.<sup>[20–27]</sup> One of the simplest approaches to control the primary chain dispersity is to use reversible addition-fragmentation chain transfer polymerization (RAFT) with chain transfer agents of different activities.<sup>[23,28,29]</sup> In RAFT, the chain transfer agent (CTA) is typically a thiocarbonylthio compound that mediates the polymerization by reacting with the propagating radical to generate the RAFT intermediate radical.<sup>[16,28,30]</sup> This can subsequently fragment, leading to the exchange of the polymer chain capped with the CTA and the propagating polymer radical. Dispersity of the previously linear polymer, or primary chain, can be modulated in RAFT by choosing combinations of more and less active CTAs.<sup>[16,31]</sup> The more active CTA leads to shorter transient radical lifetimes before degenerate exchange, resulting in narrower distributions, while a less active CTA causes longer transient radical lifetimes and thereby forms broader distributions.<sup>[24,25,32]</sup> Combinations of more and less active CTAs, lead to intermediate dispersities.<sup>[31,32]</sup>

The wealth of polymerization methods that can control dispersity, introduces the opportunity for materials properties to be engineered. Important results highlight perturbations of block copolymer self-assembly tuned by dispersity of the linear chains. This has been predicted by theoretical approaches,<sup>[33,34]</sup> and realized through a series of detailed

## Introduction

The molecular structure of a macromolecule is intimately tied to the performance of the polymeric material in a given application.<sup>[1–3]</sup> Changes in branching and molecular weight can alter the properties and applications of polymers. For

[\*] I. O. Raji, Dr. O. J. Dodo, Dr. N. K. Saha, M. Eisenhart, Prof. Dr. D. Konkolewicz  
 Department of Chemistry and Biochemistry, Miami University, Oxford, Ohio 45056, USA  
 E-mail: d.konkolewicz@miamioh.edu  
 Prof. Dr. K. M. Miller  
 Department of Chemistry, Murray State University, Murray, KY 42071, USA

Dr. R. Whitfield, Prof. Dr. A. Anastasaki  
 Laboratory of Polymeric Materials, Department of Materials, ETH Zurich, Vladimir-Prelog-Weg 5, Zurich, Switzerland

© 2024 The Authors. Angewandte Chemie International Edition published by Wiley-VCH GmbH. This is an open access article under the terms of the Creative Commons Attribution Non-Commercial License, which permits use, distribution and reproduction in any medium, provided the original work is properly cited and is not used for commercial purposes.

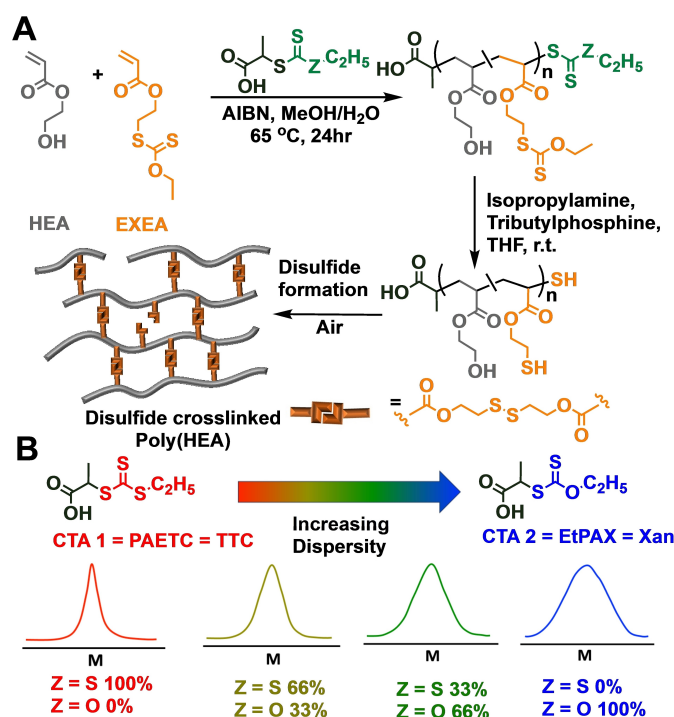
block copolymer self-assembly studies,<sup>[35–37]</sup> before being translated to thermoplastic elastomers after block copolymer assembly.<sup>[38,39]</sup> However, the effect of primary chain dispersity on covalently crosslinked networks has received limited attention, despite the fact that covalent crosslinked polymers comprise the largest fraction of thermosetting and elastomeric materials.<sup>[40]</sup> This implies that controlling backbone chain dispersity is an untapped resource to control bulk material properties. In the past decades, the Macosko group has done extensive theoretical and experimental studies to investigate the effects of polymer molecular weight on the behavior of polymer networks.<sup>[41–43]</sup> These studies were primarily done on poly(dimethyl siloxane) but generally established the fundamentals to understanding the relationship between polymer molecular weight and network properties.<sup>[41–46]</sup> Also, studies in the past decade have established the significant influence of molecular weight distribution on the properties of rubber and plastic polymers. Roland and colleagues investigated the role of molecular weight distribution on the network formation and rheology in monodisperse and polydisperse 1,4-polybutadienes.<sup>[44]</sup> Their study revealed that molecular weight distribution affects polymer gelation, with the gelation point observed for lower crosslinking degrees as MWD increases. They also showed that the effect of formation of polymer networks on the mechanical properties largely hinges on the molecular weight distribution. Needless to say, the importance of MWD on mechanical properties cannot be overemphasized.<sup>[47–49]</sup> Recently, Weems and co-workers<sup>[50]</sup> developed a ring-opening polymerization approach to control primary backbone dispersity, with subsequent functionalization to create cross-linkable monomers. Although demonstrating changes in mechanical properties with different backbone dispersity, the materials synthesized also had substantial differences in number averaged molecular weight coupled with the changes in dispersity, making separation of the chain length and dispersity effects challenging. Similarly, Sumerlin and co-workers<sup>[51]</sup> highlighted how blending polymers leading to complex molecular weight distributions with distinct dispersity and skew, lead to control over creep rates and activation energies in dynamic materials. However, the exploration of bulk mechanical properties as a function of primary chain dispersity was not performed in this study. Here, the primary chain dispersity is systematically varied using a RAFT approach, and the impact of these primary chain effects on bulk materials' mechanical properties is investigated. Additionally, taking advantage of facile processing, adhesive properties of these materials was explored. Combined, these studies highlight how systematic control over primary chain dispersity could be used in future applications that focus on polymers for structural, elastic, or adhesive applications.

## Results and Discussion

Poly (hydroxyethyl acrylate) (Poly-HEA) networks were synthesized with tunable primary chain length and backbone dispersity using a modification of the mixed chain transfer

agent (CTA) RAFT polymerization approach developed in the literature.<sup>[31,32,52]</sup> A more active trithiocarbonate (TTC) CTA and a less active Xanthate (Xan) CTA were combined in different ratios to give polymers of tunable dispersity. Scheme 1A displays the synthesis of polymer networks, and Scheme 1B highlights how mixtures of more active TTC and less active Xan CTAs can give polymers of tunable dispersity. Four ratios of CTAs were used, TTC:Xan = 100:0, 67:33, 33:67 and 0:100. In each system a constant ratio of HEA to the protected thiol crosslinker EXEA (Scheme 1) of HEA:EXEA = 100:6, or equivalently 200:12 was used. This is anticipated to give a consistent spacing of crosslinkers along the backbone and similar mesh sizes for each system.

The mixed CTA in RAFT polymerization not only gave polymers with predictable number averaged molecular weights close to the ratio of monomer to total CTA, but also provided tunable dispersity. In all cases monomer conversion was over 95 % (Figure S2). Figure 1 illustrates the molecular weight distributions for polymers targeting two distinct chain lengths: 100 (depicted in Figure 1A) and 200 (represented in Figure 1B). As indicated in Table 1 and Table S1, the primary chain molecular weight, determined by NMR analysis closely aligns with the primary chain molecular weight predicted by the ratio of monomers to total CTA, and with the targeted ratio of HEA:EXEA. When employing 100 % TTC, the polymers exhibit lower dispersity, ranging from 1.2 to 1.4, depending on the chain length. As the xanthate concentration increases, the dispersity gradually rises, eventually reaching ~2–3 for 100 % Xan.



**Scheme 1.** A) Synthesis of poly(HEA) disulfide crosslinked networks with mixed RAFT agents. B) Tuning the primary polymer dispersity using mixtures of trithiocarbonate (TTC) and xanthate (Xan) CTAs.

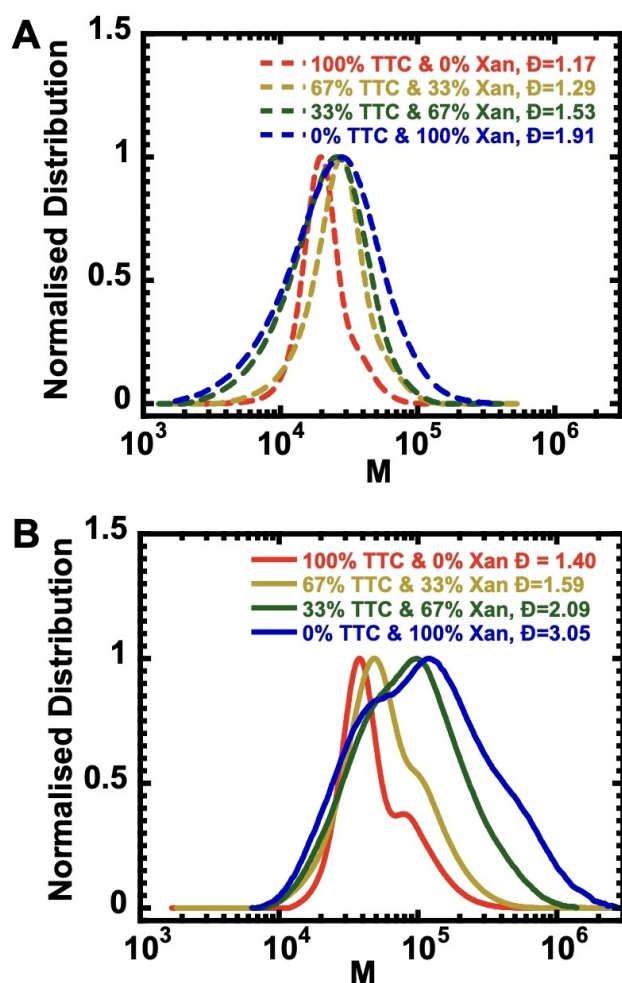


**Figure 1.** SEC traces of poly(HEA-EXEA) synthesized with ratios of TTC:Xan CTAs of 100:0, 67:33, 33:67 and 0:100 at a target DP of 100 (A) or 200 (B).

There are evidence of branching from SEC, especially at the higher primary chain length (Figure 1B), presumably due to the ethylene glycol diacrylate impurity that is common in HEA.<sup>[53]</sup> Deconvolution of the peaks<sup>[54]</sup> shown in Figure S2 suggests that the primary chain length is essentially constant in molecular weight. Although the primary chain's distribution (at lowest molecular weight by deconvolution) typically

broadens as the ratio of TTC:Xan decreases, the higher molecular weight peaks in the deconvolution are consistent with branched and multiply coupled chains from the presence of the ethylene glycol diacrylate impurity common in HEA. Therefore, despite the branching, the primary chain dispersity increases as would be expected for the ratios of TTC:Xan.

Having established that the primary chain dispersity can be varied by mixing CTAs, the thiol groups were liberated by an amine-based deprotection, and the material was crosslinked by taking advantage of the spontaneous transformation of thiols to disulfides in the presence of oxygen, resulting in elastomeric network materials. Infrared spectra of the generated networks are given in Figure S4, and they indicate essentially no evidence of free thiol peaks which typically appear at  $\sim 2600\text{ cm}^{-1}$ .<sup>[55]</sup>

Glass transition temperatures ( $T_g$ ) were measured by differential scanning calorimetry, and determined as the inflection point of the heat flow curve as outlined in the Supporting Information.<sup>[56]</sup> Table 1 and also Table S1 show that the materials have  $T_g$  at or below room temperature, consistent with soft elastomeric structures, with no statistically significant difference in  $T_g$  in the chain length 100 (one way ANOVA P-value $\sim 0.1$ ) or chain length 200 systems (one way ANOVA P-value $\sim 0.3$ ). The  $T_g$  measured by DSC shows sample to sample variability in the range of 2–6 °C, which is perhaps in part due to the fact that HEA polymers can absorb some water from the atmosphere, leading to a small extent of plasticization. Nevertheless, the elastomeric nature of the materials at ambient temperature is reflected in the plateau modulus ( $E'$ ) data reported in Table S1 and Figure S4. However, neither the  $T_g$  nor the plateau rubbery modulus had any systematic trend with respect to the primary chain dispersity, with the largest variations being sample to sample.

The equilibrium swelling ratio ( $Q$ ) was evaluated for each of the polymers synthesized and is shown in Figure 2. Interestingly, the swelling ratio reaches a peak at intermediate primary chain dispersity. Systems with either 100% TTC or 100% Xan CTA had measurably lower swelling ratios than those with intermediate dispersity, generated using either 67% TTC and 33% Xan or 33% TTC and 67% Xan ( $\bar{D}\sim 1.3\text{--}1.5$  for DP 100 and 1.6–2.1 for DP 200). Single factor ANOVA was performed for each chain length. At primary chain length of 100 units, the P-value was  $6\times 10^{-6}$ , and at

**Table 1:** Molecular weight, dispersity, thermal and tensile stress–strain data for the various synthesized poly(HEA-EXEA).<sup>[a]</sup> Young's modulus was determined from the Ogden model applied to tensile stress–strain data.

TTC:Xan	Target DP	$M_{n-Th}$ (Da)	$M_{n-NMR}$ (Da)	$\bar{D}$	$T_{g-DSC}$ (°C)	$Q$ (–)	$\sigma_{peak}$ (MPa)	$\epsilon_{break}$ (mm/mm)	$Y$ (MPa)
100:0	100	$1.31\times 10^4$	$1.37\times 10^4$	1.17	$-3\pm 3$	$0.9\pm 0.1$	$0.29\pm 0.06$	$0.5\pm 0.1$	$0.8\pm 0.2$
67:33	100	$1.31\times 10^4$	$1.22\times 10^4$	1.29	$-8\pm 4$	$1.31\pm 0.02$	$0.41\pm 0.09$	$0.63\pm 0.09$	$1.0\pm 0.2$
33:67	100	$1.31\times 10^4$	$1.27\times 10^4$	1.53	$-4\pm 2$	$1.45\pm 0.02$	$0.4\pm 0.1$	$0.7\pm 0.1$	$0.9\pm 0.1$
0:100	100	$1.31\times 10^4$	$1.39\times 10^4$	1.91	$5\pm 6$	$1.06\pm 0.04$	$0.3\pm 0.1$	$0.3\pm 0.1$	$1.5\pm 0.3$
100:0	200	$2.61\times 10^4$	$2.45\times 10^4$	1.40	$-3\pm 6$	$1.3\pm 0.2$	$0.51\pm 0.07$	$0.6\pm 0.1$	$1.3\pm 0.1$
67:33	200	$2.61\times 10^4$	$2.47\times 10^4$	1.59	$4\pm 4$	$1.79\pm 0.06$	$0.7\pm 0.1$	$0.6\pm 0.1$	$1.7\pm 0.1$
33:67	200	$2.61\times 10^4$	$2.48\times 10^4$	2.09	$-4\pm 2$	$1.8\pm 0.1$	$0.8\pm 0.1$	$0.9\pm 0.1$	$1.48\pm 0.06$
0:100	200	$2.61\times 10^4$	$2.39\times 10^4$	3.05	$3\pm 2$	$1.28\pm 0.03$	$0.6\pm 0.1$	$0.5\pm 0.1$	$1.52\pm 0.04$



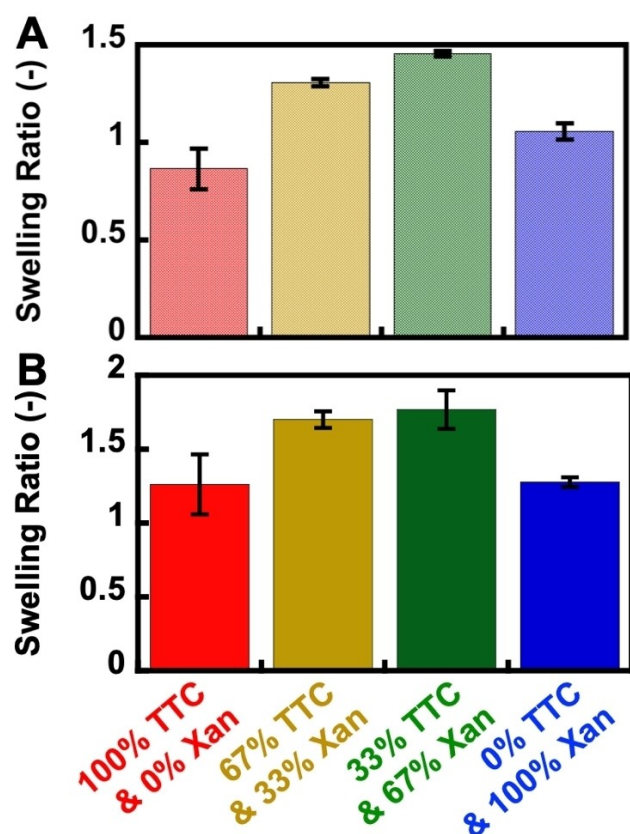


**Figure 2.** Swelling ratio of poly(HEA) based networks synthesized with ratios of TTC:Xan CTAs of 100:0, 67:33, 33:67 and 0:100 at a target DP of 100 (A) or 200 (B).

primary chain length of 200 units, the P-value was  $1 \times 10^{-3}$ , for the null hypothesis that all combinations of TTC and Xan CTAs had the same swelling ratios. This statistical analysis provides very strong evidence that control over the primary chain dispersity changes the bulk material's swelling properties.

The mechanical properties of elastomeric materials was evaluated for each chain length and backbone dispersity using tensile testing. As seen in Figure 3, the median material's stress-strain properties depend not only on the primary chain length, but also on the backbone dispersity. Intermediate dispersity ( $D \sim 1.3$ – $1.5$  for DP 100 and  $1.6$ – $2.1$  for DP 200) led to superior mechanical properties, especially in the peak stress ( $\sigma_{\text{peak}}$ ) compared to either low or high dispersity. Primary chain dispersity had a major impact on the  $\sigma_{\text{peak}}$  and to a smaller extent the strain at break ( $\epsilon_{\text{break}}$ ). In both the target chain length 100 and 200 systems, the  $\sigma_{\text{peak}}$  values were substantially higher at intermediate dispersity, formed by using either 67% of TTC with 33% Xan or 33% TTC with 67% Xan than for either the high or low dispersity materials. A similar albeit less pronounced trend was observed in  $\epsilon_{\text{break}}$ . ANOVA indicates that both the  $\sigma_{\text{peak}}$  and  $\epsilon_{\text{break}}$  are statistically significant at the 1% level for both the chain length 100 and 200 series. The P-values for equal  $\sigma_{\text{peak}}$  values across all dispersities are  $9 \times 10^{-3}$  and  $3 \times 10^{-4}$  for the primary chain length 100 and 200 series respectively.

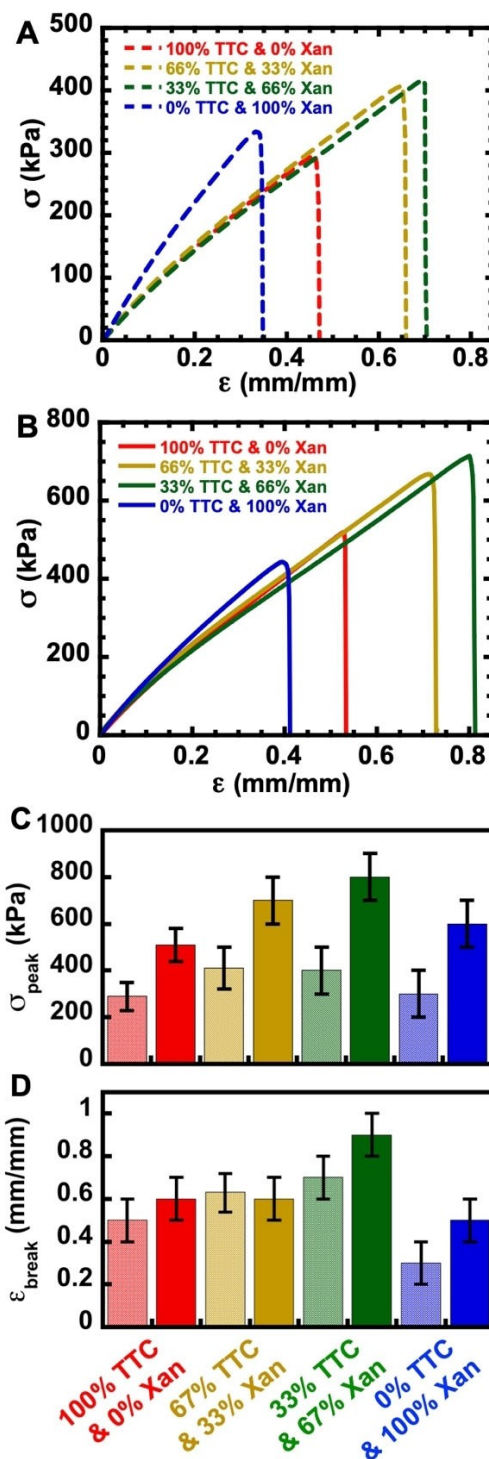


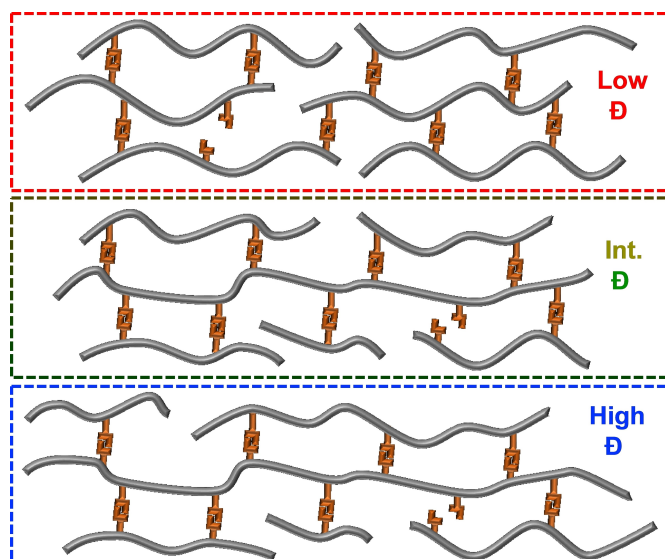
**Figure 3.** Mechanical properties of poly(HEA) based networks synthesized with ratios of TTC:Xan CTAs of 100:0, 67:33, 33:67 and 0:100. Median stress-strain curves at a target DP of 100 (A) or 200 (B). Mean peak stress ( $\sigma_{\text{peak}}$ ) C and Mean strain at break ( $\epsilon_{\text{break}}$ ) D. In C and D, light-shaded bars correspond to target DP of 100, and solid bars correspond to target DP of 200.

Similarly, the P-values for equal  $\epsilon_{\text{break}}$  for all primary chain dispersities are  $6 \times 10^{-5}$  and  $3 \times 10^{-4}$  for the primary chain length 100 and 200 series, respectively. In general, the

Young's modulus only showed a relatively minor change in properties as the primary chain dispersity was varied (Table 1). There was a systematic increase in modulus going from target chain length of 100 to 200, consistent with the theory of rubber elasticity as highlighted in the Supporting Information.<sup>[57]</sup> Beyond that however, the slope of the stress-strain curve was weakly affected by the primary chain dispersity.

Surprisingly, a network comprised of highly uniform chains does not lead to the best mechanical properties (Figure 3), nor the highest swelling (Figure 2), but instead, materials based on intermediate dispersity lead to the best network properties. This can be defined as strongest materials or materials most capable of swelling with solvent, which has been connected to overall network uniformity.<sup>[14,58]</sup> Indeed, this is an unusual result, because in general RDRP methods lead to more uniform networks than their FRP counterparts due to the control over the primary chain structure.<sup>[14,59–62]</sup> This highlights the importance of control over the primary chain dispersity when designing polymer materials. A possible reason for the enhanced material properties at intermediate primary chain dispersity when compared to either high or low dispersity systems is given in Scheme 2. Intermediate dispersity systems have some longer chains, which can better connect distinct parts of the network together, enhancing network percolation. In contrast, lower dispersity systems have fewer opportunities for one polymer to link to several adjacent chains. In contrast, the high dispersity system has a mixture of effective long chains, but also many shorter chains that are bonded to the network, but not able to entangle or form crosslinks that percolate the network.

Finally, the various primary chain dispersity networks were tested in adhesive applications as given in Figure 4, measured by lap shear analysis using pine substrates. When considering the target chain length of 100, the adhesive



**Scheme 2.** Schematic illustration of how the network structure changes as the primary chain dispersity ( $\bar{D}$ ) increases.

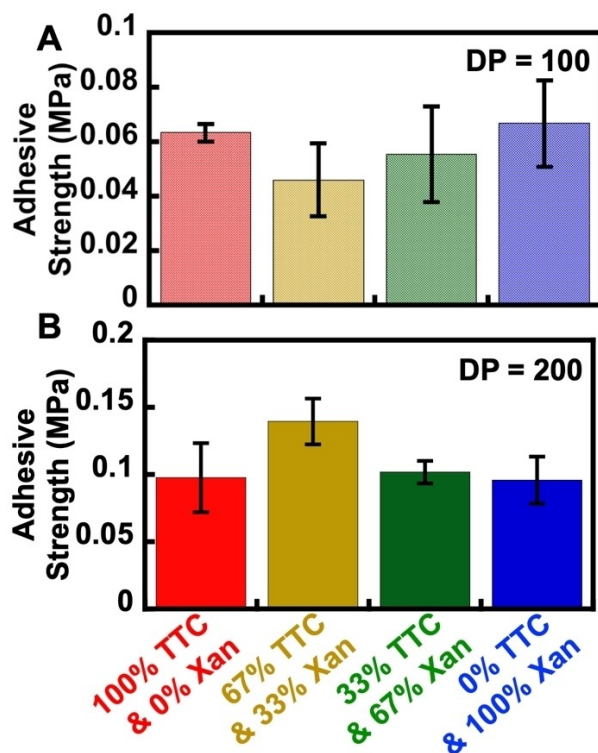


**Figure 4.** Adhesive strength of poly(HEA) based networks synthesized with ratios of TTC:Xan CTAs of 100:0, 67:33, 33:67 and 0:100. A) Target DP = 100, B) Target DP = 200.

strength to pine substrates was relatively low (typically below 60 kPa), and ANOVA tests showed little variation between the polymer compositions, with a P-value of 0.32. With target chain length of 200, the adhesive strength was higher (~100 kPa) for all the samples and this resulted in greater consistency in measurement. Significantly, the moderate dispersity sample with 67% TTC had a substantially higher adhesive strength to the pine substrate, compared to all the other network structures. ANOVA testing gave a P-value of 0.056, which is close to statistically significant, and could be due to the relatively small number of replicates (triplicate for each sample). The adhesive strengths of the DP=200 polymers are broadly consistent with the tensile analysis.

The overall results indicate that both chain length and dispersity play pivotal roles in the material properties. This is even in systems with otherwise the same crosslink density. Although chain length effects have been well reported in the literature,<sup>[63–66]</sup> this work provides a clear indication of how primary chain dispersity can be used to increase a material's swelling, strength, extensibility and adhesive properties.

## Conclusions

In conclusion, disulfide-crosslinked poly(HEA-EXEA) elastomers were synthesized, and the dispersity of polymer materials were tuned by mixing a more active trithiocarbonate (TTC) CTA and a less active Xanthate (Xan) CTA in

different ratios. This resulted in polymers with low, intermediate and high dispersity values. The intermediate dispersity polymers showed improved mechanical properties, swelling behavior and adhesive strength compared to the low and high primary chain dispersity polymers. The polymers showed no significant differences in terms of thermal properties. Overall, this work highlights how systematic control of polymer dispersity is integral to the performance of the material in a variety of applications targeting structural, elastomeric or hydrogel type applications. Careful design of polymers with intermediate dispersity can lead to enhanced strength, swelling, and potentially tunable adhesion, superior to the extremely low or high dispersity materials.

### Author Contributions

I.O.R. was involved in experimental design, synthesis of polymers, data analysis, visualization, writing, and editing of the manuscript. O.J.D. was involved in experimental design, validation, and analysis. N.K.S. was involved in synthesis, design of polymers, and molecular weight analysis. M.E. was involved in formal and statistical analysis. K.M.M. was involved in dynamic mechanical analysis. R.W. was involved in conceptualization, editing and analysis. A.A. was involved in conceptualization, editing, and analysis. D.K. was involved in conceptualization, experimental design, formal analysis, visualization and writing.

### Acknowledgements

This work was supported by United States Department of Energy, Office of Science, Basic Energy Sciences, under Award No. DE-SC0018645 for network synthesis and characterization of tensile, adhesive, and swelling properties.

### Conflict of Interest

The authors declare no conflicts.

### Data Availability Statement

The data that support the findings of this study are openly available in Miami University Scholarly Commons at <http://hdl.handle.net/2374.MIA/6919>, reference number 6919.

**Keywords:** Polymer Dispersity · Polymer Networks · Network structure · Mechanical properties · Adhesive Properties

- [1] Y. Gu, J. Zhao, J. A. Johnson, *Trends Chem.* **2019**, *1*, 318–334.  
 [2] S. J. Garcia, *Eur. Polym. J.* **2014**, *53*, 118–125.  
 [3] P. Maji, K. Naskar, *J. Appl. Polym. Sci.* **2022**, *139*, DOI 10.1002/app.52942.

- [4] P. Oblak, J. Gonzalez-Gutierrez, B. Zupančič, A. Aulova, I. Emri, *Polym. Degrad. Stab.* **2015**, *114*, 133–145.  
 [5] L. A. Pinheiro, M. A. Chinelatto, S. V. Canevarolo, *Polym. Degrad. Stab.* **2004**, *86*, 445–453.  
 [6] Y. M. Kim, J. K. Park, *J. Appl. Polym. Sci.* **1996**, *61*, 2315–2324.  
 [7] P. S. Eselem Bungu, H. Pasch, *Polym. Chem.* **2018**, *9*, 1116–1131.  
 [8] S. Ronca, in *Brydson's Plastics Materials: Eighth Edition*, Elsevier Inc., **2017**, pp. 247–278.  
 [9] Y. M. Kim, J. K. Park, *J. Appl. Polym. Sci.* **1996**, *61*, 2315–2324.  
 [10] M. B. Sims, *Polym. Int.* **2021**, *70*, 14–23.  
 [11] K. Matyjaszewski, in *Progress in Polymer Science (Oxford)*, **2005**, pp. 858–875.  
 [12] N. Corrigan, K. Jung, G. Moad, C. J. Hawker, K. Matyjaszewski, C. Boyer, *Prog. Polym. Sci.* **2020**, *111*, DOI 10.1016/j.progpolymsci.2020.101311.  
 [13] A. Gregory, M. H. Stenzel, *Progress in Polymer Science (Oxford)* **2012**, *37*, 38–105.  
 [14] S. V. Wanasinghe, M. Sun, K. Yehl, J. Cuthbert, K. Matyjaszewski, D. Konkolewicz, *ACS Macro Lett.* **2022**, *11*, 1156–1161.  
 [15] T. Shimizu, R. Whitfield, G. R. Jones, I. O. Raji, D. Konkolewicz, N. P. Truong, A. Anastasaki, *Chem. Sci.* **2023**, *14*, 13419–13428.  
 [16] K. G. E. Bradford, L. M. Petit, R. Whitfield, A. Anastasaki, C. Barner-Kowollik, D. Konkolewicz, *J. Am. Chem. Soc.* **2021**, *143*, 17769–17777.  
 [17] K. G. E. Bradford, V. C. Kirinda, E. A. Gordon, C. S. Hartley, D. Konkolewicz, *Macromol. Rapid Commun.* **2023**, DOI 10.1002/marc.202300094.  
 [18] K. Tao, D. Lu, R. Bai, H. Li, L. An, *Macromol. Rapid Commun.* **2008**, *29*, 1477–1483.  
 [19] O. J. Dodo, I. O. Raji, I. J. Arny, C. P. Myers, L. Petit, K. Walpita, D. Dunn, C. J. Thrasher, D. Konkolewicz, *RSC Applied Polymers* **2023**, DOI 10.1039/d3lp00012e.  
 [20] W. A. Braunecker, K. Matyjaszewski, *Progress in Polymer Science (Oxford)* **2007**, *32*, 93–146.  
 [21] D. Liu, A. D. Sponza, D. Yang, M. Chiu, *Angew. Chem. Int. Ed.* **2019**, *58*, 16210–16216.  
 [22] V. Yadav, N. Hashmi, W. Ding, T. H. Li, M. K. Mahanthappa, J. C. Conrad, M. L. Robertson, *Polym. Chem.* **2018**, *9*, 4332–4342.  
 [23] M. N. Antonopoulou, R. Whitfield, N. P. Truong, A. Anastasaki, *Eur. Polym. J.* **2022**, *174*, DOI 10.1016/j.eurpolymj.2022.111326.  
 [24] R. Whitfield, N. P. Truong, D. Messmer, K. Parkatzidis, M. Rolland, A. Anastasaki, *Chem. Sci.* **2019**, *10*, 8724–8734.  
 [25] D. T. Gentekos, L. N. Dupuis, B. P. Fors, *J. Am. Chem. Soc.* **2016**, *138*, 1848–1851.  
 [26] R. Whitfield, N. P. Truong, A. Anastasaki, *Angew. Chem. Int. Ed.* **2021**, *60*, 19383–19388.  
 [27] R. Whitfield, K. Parkatzidis, M. Rolland, N. P. Truong, A. Anastasaki, *Angew. Chem. Int. Ed.* **2019**, *58*, 13323–13328.  
 [28] S. Perrier, *Macromolecules* **2017**, *50*, 7433–7447.  
 [29] G. Moad, E. Rizzardo, S. H. Thang, in *Chem Asian J*, **2013**, pp. 1634–1644.  
 [30] N. P. Truong, G. R. Jones, K. G. E. Bradford, D. Konkolewicz, A. Anastasaki, *Nat Rev Chem* **2021**, *5*, 859–869.  
 [31] R. Whitfield, K. Parkatzidis, N. P. Truong, T. Junkers, A. Anastasaki, *Chem* **2020**, *6*, 1340–1352.  
 [32] K. Parkatzidis, N. P. Truong, M. N. Antonopoulou, R. Whitfield, D. Konkolewicz, A. Anastasaki, *Polym. Chem.* **2020**, *11*, 4968–4972.  
 [33] M. M. Kearns, C. N. Morley, K. Parkatzidis, R. Whitfield, A. D. Sponza, P. Chakma, N. De Alwis Watuthantrige, M. Chiu, A. Anastasaki, D. Konkolewicz, *Polym. Chem.* **2022**, *13*, 898–913.



- [34] S. Domanskyi, D. T. Gentekos, V. Privman, B. P. Fors, *Polym. Chem.* **2020**, *11*, 326–336.
- [35] N. Hnatchuk, E. Hathaway, J. Cui, X. Li, *ACS Appl. Polym. Mater.* **2022**, *4*, 7311–7320.
- [36] T. Pan, B. B. Patel, D. J. Walsh, S. Dutta, D. Guironnet, Y. Diao, C. E. Sing, *Macromolecules* **2021**, *54*, 3620–3633.
- [37] W. Cai, S. Yang, L. Zhang, Y. Chen, L. Zhang, J. Tan, *Macromolecules* **2022**, *55*, 5775–5787.
- [38] M. Robertson, A. Guillen-Obando, A. Barbour, P. Smith, A. Griffin, Z. Qiang, *Nat. Commun.* **2023**, *14*, DOI 10.1038/s41467-023-36362-x.
- [39] M. Steube, T. Johann, R. D. Barent, A. H. E. Müller, H. Frey, *Prog. Polym. Sci.* **2022**, *124*, DOI 10.1016/j.progpolymsci.2021.101488.
- [40] C. K. Varnava, C. S. Patrickios, *Polymer (Guildf)* **2021**, *215*, DOI 10.1016/j.polymer.2020.123322.
- [41] D. R. Miller, C. W. Macosko, *J. Polym. Sci. Polym. Phys. Ed.* **1988**, *26*, 1–54.
- [42] D. R. Miller, C. W. Macosko, *J. Polym. Sci. Polym. Phys. Ed.* **1987**, *25*, 2441–2469.
- [43] S. A. Bidstrup, C. W. Macosko, *J. Polym. Sci. Polym. Phys. Ed.* **1990**, *28*, 691–709.
- [44] M. J. Schroeder, C. M. Roland, *Macromolecules* **2002**, *35*, 2676–2681, DOI 10.1021/ma011678h
- [45] C. W. Macosko, *Br. Polym. J.* **1985**, *17*, 239–245.
- [46] M. Gottlieb, C. W. Macosko, T. C. Lepsch, *Journal of polymer science. Part A-2, Polymer physics* **1981**, *19*, 1603–1617.
- [47] Juliani, L. A. Archer, *J Rheol (N Y N Y)* **2001**, *45*, 691–708.
- [48] J. van Meerveld, *J Nonnewton Fluid Mech* **2004**, *123*, 259–267.
- [49] X. Ye, T. Sridhar, *Macromolecules* **2005**, *38*, 3442–3449.
- [50] D. Merckle, A. C. Weems, *Polym. Chem.* **2023**, DOI 10.1039/d3py00608e.
- [51] J. J. Lessard, K. A. Stewart, B. S. Sumerlin, *Macromolecules* **2022**, *55*, 10052–10061.
- [52] T. Nwoko, N. De Alwis Watuthanthrige, B. Parnitzke, K. Yehl, D. Konkolewicz, *Polym. Chem.* **2021**, *12*, 6761–6770.
- [53] E. F. Gomez, S. V. Wanasinghe, A. E. Flynn, O. J. Dodo, J. L. Sparks, L. A. Baldwin, C. E. Tabor, M. F. Durstock, D. Konkolewicz, C. J. Thrasher, *ACS Appl. Mater. Interfaces* **2021**, *13*, 28870–28877.
- [54] N. De Alwis Watuthanthrige, J. A. Reeves, M. T. Dolan, S. Valloppilly, M. B. Zanjani, Z. Ye, D. Konkolewicz, *Macromolecules* **2020**, *53*, 5199–5207.
- [55] Z. Kuodis, I. Matulaiienė, M. Špandyreva, L. Labanauskas, S. Stončius, O. Eicher-Lorka, R. Sadzevičienė, G. Niaura, *Molecules* **2020**, *25*, DOI 10.3390/molecules25235633.
- [56] P. Chakma, L. H. Rodrigues Possarle, Z. A. Digby, B. Zhang, J. L. Sparks, D. Konkolewicz, *Polym. Chem.* **2017**, *8*, 6534–6543.
- [57] L. R. G. Treloar, *Reports on progress in physics* **1973**, *36*, 755, DOI 10.1088/0034-4885/36/7/001
- [58] S. V. Wanasinghe, E. M. Schreiber, A. M. Thompson, J. L. Sparks, D. Konkolewicz, *Polym. Chem.* **2021**, *12*, 1975–1982.
- [59] J. Cuthbert, S. V. Wanasinghe, K. Matyjaszewski, D. Konkolewicz, *Macromolecules* **2021**, *54*, 8331–8340.
- [60] C. W. A. Bainbridge, A. Wangsadijaya, N. Broderick, J. Jin, *Polym. Chem.* **2022**, *13*, 1484–1494.
- [61] F. Dawson, H. Jafari, V. Rimkevicius, M. Kopeć, *Macromolecules* **2023**, *56*, 2009–2016.
- [62] E. Mehravar, A. Agirre, N. Ballard, S. Van Es, A. Arbe, J. R. Leiza, J. M. Asua, *Macromolecules* **2018**, *51*, 9740–9748.
- [63] B. Zhang, N. De Alwis Watuthanthrige, S. V. Wanasinghe, S. Averick, D. Konkolewicz, *Adv. Funct. Mater.* **2022**, *32*, DOI 10.1002/adfm.202108431.
- [64] N. De Alwis Watuthanthrige, D. Dunn, M. Dolan, J. L. Sparks, Z. Ye, M. B. Zanjani, D. Konkolewicz, *ACS Appl. Polym. Mater.* **2022**, *4*, 1475–1486.
- [65] L. F. Hart, J. E. Hertzog, P. M. Rauscher, B. W. Rawe, M. M. Tranquilli, S. J. Rowan, *Nat. Rev. Mater.* **2021**, *6*, 508–530.
- [66] B. Soman, Y. K. Go, C. Shen, C. Leal, C. M. Evans, *Soft Matter* **2022**, *18*, 293–303.

Manuscript received: October 10, 2023

Accepted manuscript online: March 28, 2024

Version of record online: ■■■, ■■■

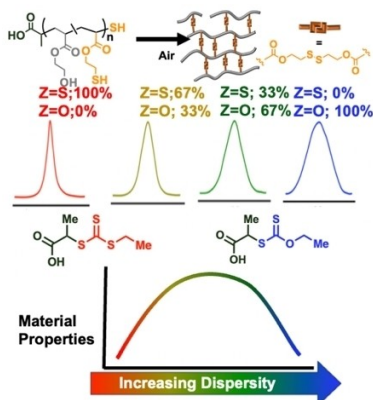


## Research Articles

## Polymer Chemistry

I. O. Raji, O. J. Dodo, N. K. Saha,  
M. Eisenhart, K. M. Miller, R. Whitfield,  
A. Anastasaki,  
D. Konkolewicz\* e202315200

Network Polymer Properties Engineered  
Through Polymer Backbone Dispersity and  
Structure



Polymer networks using chains of distinct backbone length variability were developed with control over both length and dispersity. The impact of primary chain length dispersity on material properties including strength, swelling, adhesion and extensibility were evaluated. Materials with intermediate primary chain dispersity showed superior materials properties.